Supplemental methods:

Transgenic construction

To construct the *Tg(smyhc1:lyn-tdTomato)oz29* transgenic line, we injected single cell embryos with plasmid *smyhc1:lyn-tdTomato*, described previously (Wang et al., 2011), and recovered founder lines by outcrossing injected adults and screening for fluorescent progeny. We used BAC transgenesis to generate *TgBAC(six1b:lyn-GFP)oz5*, following previously described protocols (Suster et al., 2011). Our *six1b:lyn-GFP* BAC is derived from BAC CH73-301I9, which contains *six1b*, *six4b*, and over 100 kb of surrounding sequence. We modified this BAC in three steps prior to injection. First, we replaced the first exon of *six4b* with *SpectR* to inactivate the gene, then we inserted *iTol2* sites, and finally we replaced *six1b* coding sequence with sequence encoding *lyn-GFP*. The resulting BAC *six1b:lyn-GFP-iTol2-Δsix4b* contained *lyn-GFP* at the *six1b* locus flanked by 87 kb of 3'-flanking sequence and 18 kb of 5'-flanking sequence, and no functional zebrafish genes. All modifications were sequence-confirmed, and we PCR amplified several regions of the final BAC to verify post-modification BAC integrity. We injected BAC *six1b:lyn-GFP-Tol2-Δsix4b* into one-cell zebrafish embryos together with zT2TP mRNA which encodes a zebrafish-optimized transposase (Suster et al., 2011). We raised GFP-positive embryos to adulthood and screened for germline transmission. A founder that gave rise to progeny with a lyn-GFP expression pattern closely matching that of *six1b* transcript was used to generate the *TgBAC(six1b:lyn-GFP)oz5* transgenic line.

Mutant construction and verification

Mutagenesis was performed using described protocols (Talbot and Amacher, 2014), which are available in detail online: goo.gl/xNjyNk. All lesions were sequenced initially using heterozygous DNA as a template, and all sequencing was confirmed in a subsequent generation using homozygous DNA as a template. For deletion alleles, CRISPR guide RNA (gRNA) targeting the 5' and 3' ends of the deleted region were co-injected, and embryos were screened for PCR products that span the deleted interval (Xiao et al., 2013). $met^{+13\text{-}3}$ was generated using zinc finger nucleases targeting sequences CCATGGAGCTCCAGACCGC and AGAGCTGGAGGTGGAGGT. $met^{+13\text{-}3}$ contains a 10 basepair (bp) net insertion causing a predicted frameshift beginning at amino acid 903 of 1383, prior to the transmembrane domain. $six1b^{oz1}$ contains a 14 bp net deletion causing a predicted frameshift beginning at amino acid 57 of 285. $six1b^{oz1}$ was generated using TALENs targeting sequences CCTCAAAGCCAAGGCTGTCGT and AACTTCAGGGAACTTTAT; plasmids encoding these TALENS were purchased from the University of Utah Mutation Detection and Generation core facility. $\Delta six1b^{oz34}$ deletes codons 1-259 of the 284 *six1b* codons, and removes all available ATG start codons. $\Delta six1b^{oz34}$ was generated by co-injecting two gRNAs, one targeting the 5' end of *six1b* (target: GCTTCCTTCGTAGCATCCAG) and the other targeting the 3' end of *six1b* (target: GGCGCCGCACAGTCGGTACA). $six4a^{oz40}$ contains a 5 bp deletion causing a predicted frameshift at amino acid 55 of 594 and was generated using gRNA targeting the sequence GGGCCAGCAGACCTCTCCAC. $six4b^{oz35}$ contains an 11 bp insertion that causes a predicted frameshift after amino acid 21 of 615 and was generated using gRNA targeting the sequence GGCACTAATGACCTCGCTTG. To generate double mutants that frameshift both *six1b* and *six4b*, we generated a second *six4b* allele, $six4b^{oz31}$, in fish already carrying the $six1b^{oz1}$ mutation, using gRNA targeting the sequence GTACAAGGCGCGCTACACCG. $six4b^{oz31}$ contains a 5 bp deletion causing a predicted frameshift after amino acid 146 of 615. Genotyping confirms that in crosses of $six1b^{oz1}$;$six4b^{oz31}$ carriers, all progeny co-segregate both mutant or both wild-type alleles (0 crossovers in 160 meioses). To delete both *six1b* and *six4b* we co-injected embryos with gRNA targeting the 5' end of *six4b* (target: GGCACTAATGACCTCGCTTG) and the 3' end of *six1b* (target: GGCGCCGCACAGTCGGTACA). The resulting chromosomal deficiency $Df(Chr20:six1b,six4b)^{oz16}$ (a.k.a. *Δsix1b;4b)* lacks almost all of *six1b* and *six4b*, including the homeobox sequences. To generate a deletion of both *six4a* and *six1a* we co-injected embryos with gRNA targeting the 5' end of

six4a (target: GGGCCAGCAGACCTCTCCAC) and the 3' end of *six1a* (target: GGCGCACCCAGGCCGGGCAT). The resulting chromosomal deficiency *Df(Chr13:six1a,six4a)*^{oz27} (a.k.a. *Δsix1a;4a*) lacks most of *six1a* and *six4a*, including the homeobox sequences. The *Df(Chr20:six1b,six4b)*^{oz16} and *Df(Chr13:six1a,six4a)*^{oz27} deficiencies do not entirely remove *six1/six4* coding sequences but do eliminate all annotated functional domains and are predicted to be null. We identified the *Δsix1b;4b*^{oz16} and *Δsix1a;4a*^{oz27} deletions using primers that bridge the deletion. In *Δsix1b;4b*^{oz16} and *Δsix1a;4a*^{oz27} homozygotes we fail to amplify PCR products for sequences within the deleted interval, confirming that genes are deleted. The *six4a-six1a* and *six4b-six1b* gene pairs are closely linked, and the two deletion alleles do not remove other annotated genes. Because the *Δsix1b;4b*^{oz16} deficiency phenotype closely resembles the *six1b*^{oz1};*six4b*^{oz31} double mutant phenotype, we infer that the deficiency allele reflects loss of *six1b* and *six4b* gene function.

Genotyping

Fish were genotyped using PCR amplification of DNA extracted from adult tail clip, whole embryos, or the posterior end of embryo tails, using the following primers (primer sequence indicated from 5' to 3'). For *aldh1a2*^{i26}, TGAACGAGCTCCCACAGTAA and TGTGGTCAGAATGGACAGACA; for *met*$^{+13-3}$, ACGGTGAGGTGCTGAGAGTT and GCTGGAACAAGAAGAGG; for *six1a*^{oz9}, GCACAACCACCCGAAGATG and CTCGCCGTCCCAGATAGTAC; for *six1b*^{oz1}, ATTCCGCTTCCTTCGTAGCATC and TGCAGCTTCGGGTGATTGTG; for *six1b*^{oz34}, AGTCGCGCAGTACTCTTTTAGC, TACTCCATGACCGGTCTC, and GTCGCAATCACTTAAGAGCCTAGG; for *six1b*^{oz40}, TCAAACTCCTGACTCTGGACAG and TGTGCGCAAACAAAGAGTCC; for *six4b*^{oz31}, AGAACCACTCTTTCAGCCCG and GCGTTCCGAGACCTCTCTTT; for *six4b*^{oz35}, CAGGACGCGTTCAAAATGTC and AAGTTCGGCATTCTCCATCG; for *Δsix1a;4a*^{oz27}, GCACAACCACCCGAAGATG, GTTTCCTCTAGTGAAGTGACAGTG, CTCGCCGTCCCAGATAGTAC, and ACGCACTTGTCCAGAAAACC; for *Δsix1b;4b*^{oz16}, TGGTCGCTCTCATTAATCGAAGG, AATCAAAACGCGCTCAGGAC, CCTGCGTAAACCCGAAAGAAG, and CGCAATCACTTAAGAGCCTAGG. The PCR products from *aldh1a2*^{i26}, *six1a*^{oz9}, *six1b*^{oz1}, and *six4b*^{oz31} were then digested with PstI, MnlI, MwoI, and HaeII, respectively, to distinguish wild-type from mutant PCR products. All finless embryos from *aldh1a2*^{i26} genotyped as mutant (N=30). Surprisingly, we find that the *aldh1a2*^{i26} phenotype is partially penetrant, as 2/72 embryos with fins genotyped as mutants. To genotype large deletions (*Δsix1b*^{oz34}, *Δsix1a;4a*^{oz27}, and *Δsix1b;4b*^{oz16}), we used cocktails of three to four primers that amplify across the deletion in mutants or amplify from wild-type sequences that are missing in mutants. Primer sequences available upon request. *Δsix1b;4b*^{oz16} homozygotes can also be identified beginning at 24 hpf by the severe and fully penetrant ear defect (Figure S3). For some experiments (Figure 2E, F; S4) we in-crossed *Δsix1a;4a* homozygotes that are also heterozygous for *Δsix1b;4b* resulting in a clutch where all embryos lacking both maternal and zygotic *six1a* and *six4a*, and one quarter are zygotically mutant for all *six1* and *six4* genes. We found no phenotypic difference between embryos lacking zygotic *six1a/six4a* and embryos lacking both maternal and zygotic *six1a/six4a*, consistent with data from the European Bioinformatics Institute (www.ebi.ac.uk), which shows that *six1* and *six4* transcripts are not maternally deposited.

Probe construction

To generate probes RNA in situ hybridization, we prepared cDNA from 20-26 hpf embryos, and then amplified PCR products using the following primers: *six1a*, GCTTTCTCTGTCAAATATCCATCC and CCTTAGATTCCACTTTGGTGTTTAG; *six1b*, TAATCGAAGGCAAACGGGGTG and TGGCAAATGTCAGTCCGTAATAGTC; and *six4b* GTCAAAATGCCCTCACACTCAG and TTGGGCAGATGGATGTCTTGAG. The resulting amplicons were cloned into PCR4-TOPO vectors and sequence confirmed. For mRNA synthesis, these plasmids were linearized using NotI (New

England Biolabs) then used as templates for mRNA synthesis (mMessage mMachine T3 kit; Invitrogen).

Muscle measurements and inclusion criteria

Embryos were selected randomly for confocal imaging, and all imaged embryos are included in statistical analysis. Embryos were excluded from imaging only if they appeared unhealthy under low magnification. Individual muscles were excluded if they could not be measured due to physical damage during processing or because they were not completely contained in the image's field of view. Measurements were taken on projections using the line tool in ImageJ software as described below. SHM length is the length of sternohyoideus muscle, measured on confocal z-projection. SHM lengths include measurements from both sides of the fish. We found no significant difference between left and right side SHM lengths imaged in ventral view (not shown). All other features were measured unilaterally. Fin muscle lengths were measured on confocal z-projections. AbFM and AdFM width are the widths of abductor and adductor muscles within the pectoral fin, imaged in lateral view. Because the AbFM obscures the AdFM on confocal z-projections, we measured AbFM and AdFM widths on confocal z-sections. The PHM was measured on confocal z-projection of embryos imaged in lateral view. PHM length was measured from the anterior edge that connects to the cleithrum bone to the posterior boundary with the sixth muscle segment. The posterior PHM boundary was chosen to avoid possible confusion between the PHM and myotome extensions. PHM width was measured perpendicular to PHM length. All muscles were measured across the broadest area of the appropriate axis.

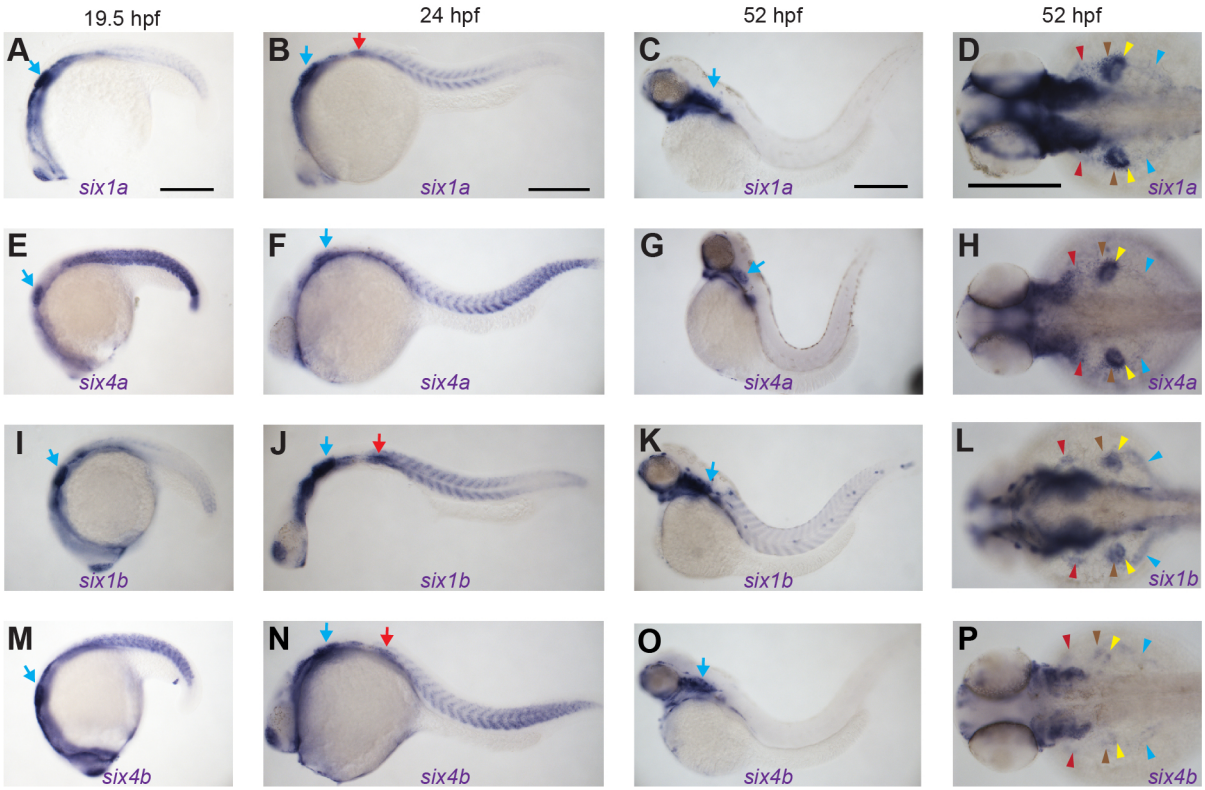

Figure S1. Overview of *six1a, six1b, six4a,* and *six4b* mRNA expression patterns. (A-P) RNA in situ hybridization for *six1a, six1b, six4a,* and *six4b* in embryos fixed at indicated times. **(A-C)** *six1a* trunk muscle expression peaks at 24 hpf and is lost by 52 hpf. **(D)** At 52 hpf, *six1a* is expressed in all MMP streams (arrowheads) and is most prominent in fin MMPs (brown and yellow arrowheads). **(E-H)** *six4a* expression is very similar to *six1a* expression in trunk muscle and MMP streams. **(I-L)** *six1b* is expressed in trunk muscle, persisting at 52 hpf, and in all MMP streams. **(M-P)** *six4b* trunk muscle expression peaks at 24 hpf and is lost by 52 hpf; at 52 hpf, *six4b* is expressed in all MMP streams. *six1*/*six4* genes are also expressed in other structures such as the ear (blue arrows) and the PrimI lateral line primordium (red arrows in *six1a*, *six1b*, and *six4b* panels). All supplemental figures use color-coded arrowheads, described also in Figure 1 legend, to indicate different MMP streams and the muscles they form. Red indicates the SHM and its precursors, brown indicates the AbFM and its precursors, yellow indicates the AdFM and its precursors, and light blue indicates the PHM and its precursors. Scale bars are 250 μm.

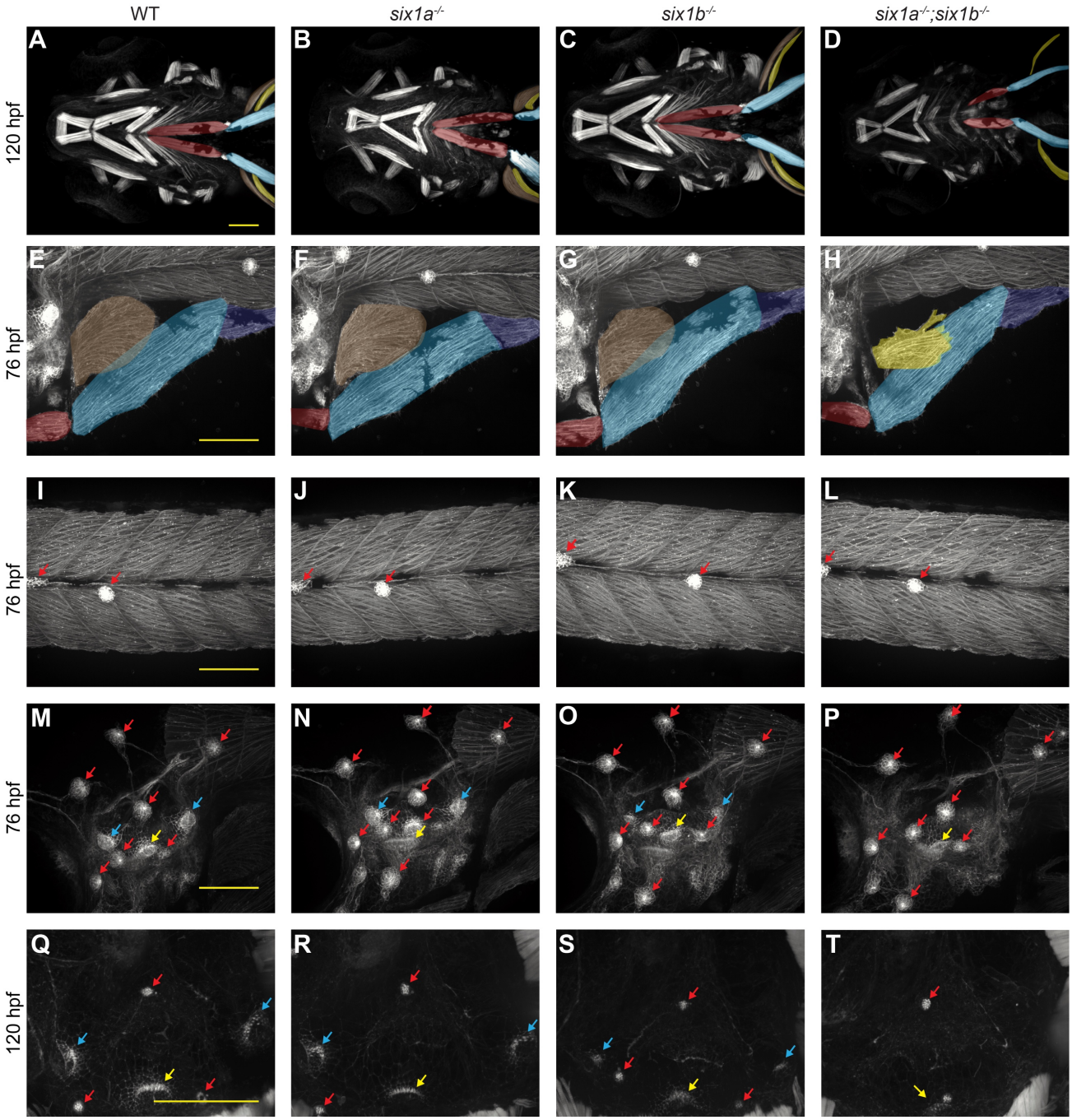

Figure S2. Together, zebrafish *six1a* and *six1b* are required for normal MMP-derived muscles and ear sensory epithelia. (A-D) Confocal projection of 120 hpf phalloidin-labeled embryos, imaged ventrally. Muscles appear normal in wild-type and single mutant embryos, but the SHM (red) is shortened and the AbFM (brown) is sometimes absent in *six1a;six1b* double mutants. In A-H, Muscles are false-colored as described in Figures 1 and S1. **(E-P)** Confocal projection of fixed 76 hpf *six1b:lyn-GFP* transgenic embryos, imaged laterally. (E-H) MMP-derived hypaxial muscles are normal in wild-type and single mutant embryos, but are reduced in *six1a;six1b* double mutants, which often lack the AbFM (brown) which normally covers the AdFM (yellow) (E-H). Trunk muscle and trunk neuromasts (red arrows) appear normal even in *six1a*;*six1b* double mutant embryos (I-L). Ear neuromasts (red arrows) are also normal in single and double mutants; however, ear cristae (blue arrows), a type of sensory epithelium, are small in *six1b* mutants and lost in *six1a;six1b* double mutants (M-P). Another ear sensory epithelium, the ventral macula (yellow arrows), is present even in double mutants. **(Q-T)** Ear cristae defects are also apparent in confocal sections of 120 hpf phalloidin-labeled embryos. All scale bars are 100 μm.

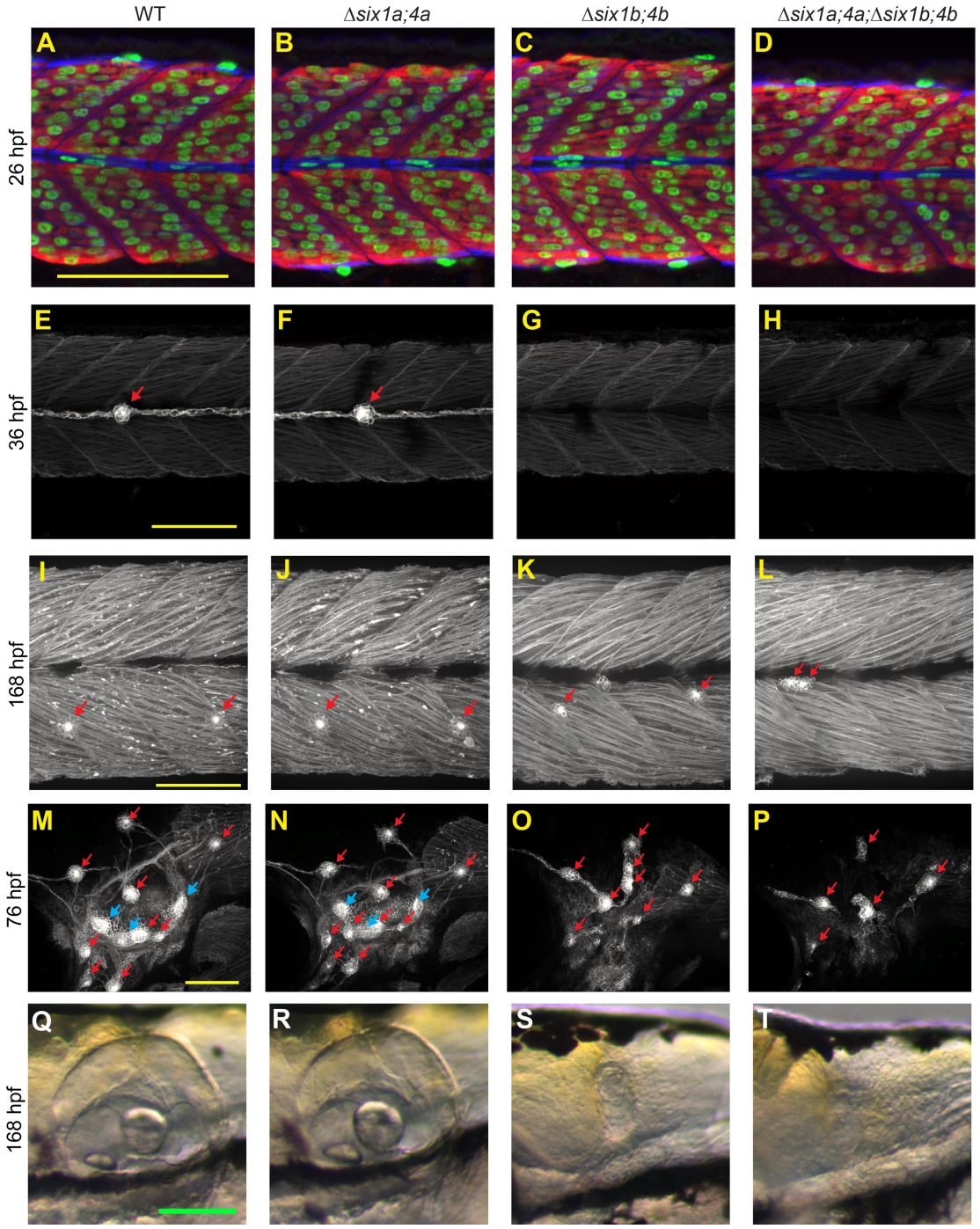

Figure S3. *six1b/six4b* function is essential for lateral line and ear formation. (A-D) Trunk muscle at 26 hpf, labeled for myosin heavy chain marker A4.1025 (blue), the myosin light chain marker F310 (red), and the myonuclei marker Rbfox1l (green). Both slow and fast muscle morphology appears normal in *six* family compound mutants. **(E-P)** Confocal projections of *six1b:lyn-GFP* transgene-expressing embryos. At 36 hpf, the lateral line and neuromasts (red arrows) are absent in the trunk of *Δsix1b;4b* homozygotes and *Δsix1a;4a;Δsix1b;4b* mutants (E-H); however, neuromast development partially and variably recovers by 7 days post fertilization (I-L). In WT and *Δsix1a;4a* mutants, the ear maculae and cristae are marked by the *six1b:lyn-GFP* transgene (green arrows); these ear sensory epithelia are lost in *Δsix1b;4b* homozygotes and *Δsix1a;4a;Δsix1b;4b* mutants (M-P). While head neuromasts (red arrows) persist in these mutants, they are mis-localized within the region where the ear would normally form. **(Q-T)** Live brightfield images showing ear morphology in wild-type and *six* family compound mutant embryos at 168 hpf. All scale bars are 100 μm.

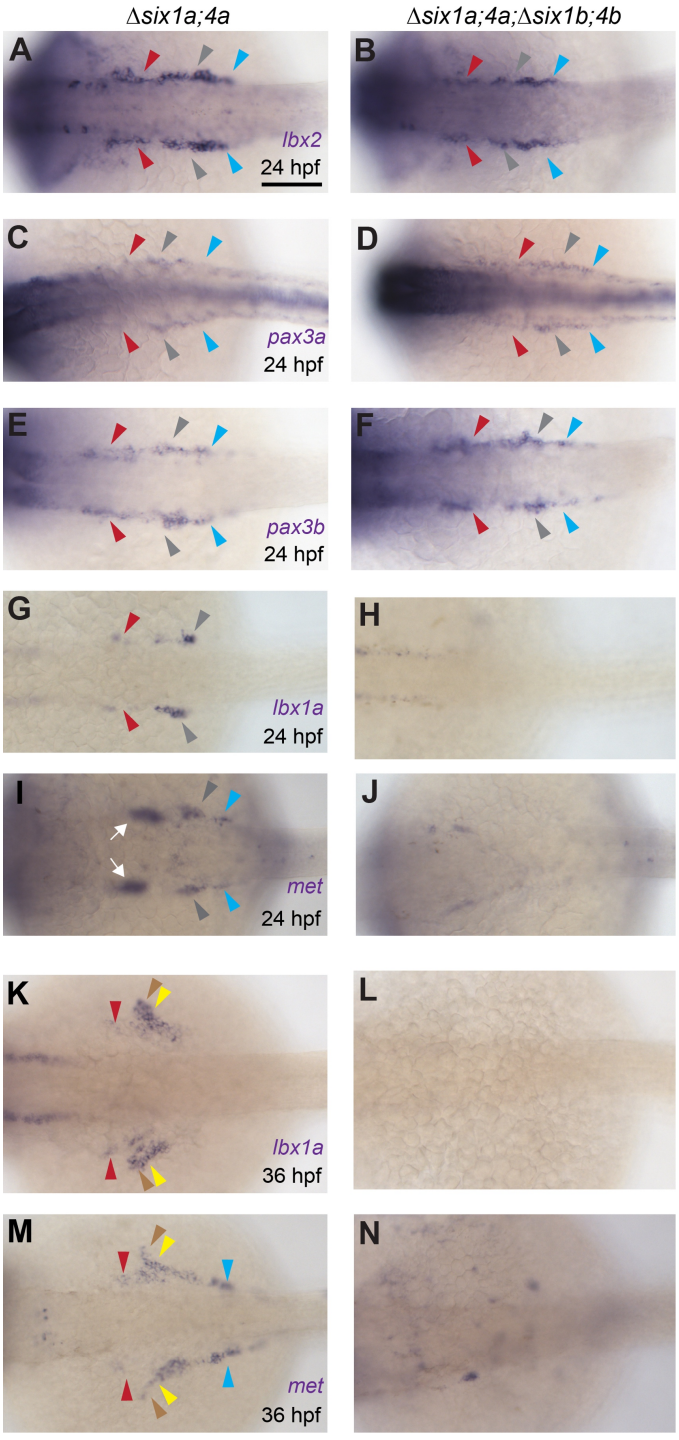

Figure S4. *six1/six4* genes are required for full MMP specification. RNA in situ hybridization of *Δsix1a;4a* mutants (left column) or *Δsix1a;4a;Δsix1b;4b* mutants (right column) fixed at **(A-J)** 24 hpf or **(K-N)** 36 hpf. Arrowheads point to MMPs and MMP-like cells. For all MMP markers tested, *Δsix1a;4a*$^{-/-}$ embryos show wild-type expression. Compared to controls, *Δsix1a;4a;Δsix1b;4b* mutants show normal (A, B) *lbx2*, (C, D) *pax3a*, and (E, F) *pax3b* gene expression at 24 hpf (A-F). However, *Δsix1a;4a;Δsix1b;4b* mutants lack *lbx1a* and *met* gene expression in MMPs at (G-J) 24 hpf and (K-N) 36 hpf. At 24 hpf, arrowhead color is assigned based on somite count: arrowheads pointing to somite 2 are red, somite 4 is gray, and somite 5 is light blue. At 36 hpf, arrowhead color is assigned based on stream shape and corresponds to that described in Figures 1 and S1. Expression of *met* in lateral line primordia is indicated by white arrows. Scale bar is 100 *μ*m.

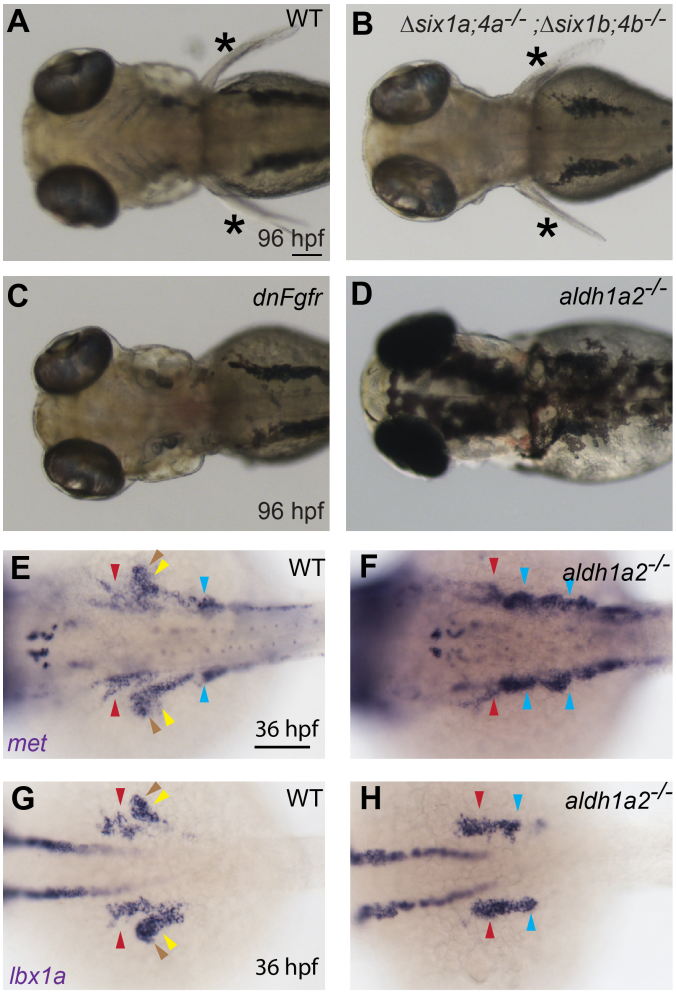

Figure S5. Fins are not required for MMP specification. (A-D) Brightfield images of four-day-old embryos. Brightfield images of wild-type, dnFgfr-expressing, and *Δsix1a;4a;Δsix1b;4b* mutant embryos. Fins are present (asterisk) in wild-type (A) and *Δsix1a;4a;Δsix1b;4b* mutant (B) embryos, but absent in dnFgfr-induced (C) and *aldh1a2* mutant (D) embryos (*aldh1a2* mutant fin phenotype previously shown by Grandel et al., 2002). **(E-J)** RNA in situ hybridization for **(E, F)** *met* and **(G, H)** *lbx1a* in 36 hpf embryos. **(E-H)** Although migratory streams are severely misshapen in *aldh1a2* mutants, MMP markers *lbx1a* (E, F) and *met* (G, H) are expressed at levels comparable to wild-type embryos. In *aldh1a2*$^{-/-}$ mutant MMPs, *met* expression appears darker than in WT (E, F); this may be due to greater cell density in the mutant, which has impaired migration. Embryos in A-C and E-H were PTU-treated to inhibit pigment formation. MMP arrowheads are color coded as described in Figures 1 and S1. Scale bars are 100 μm.

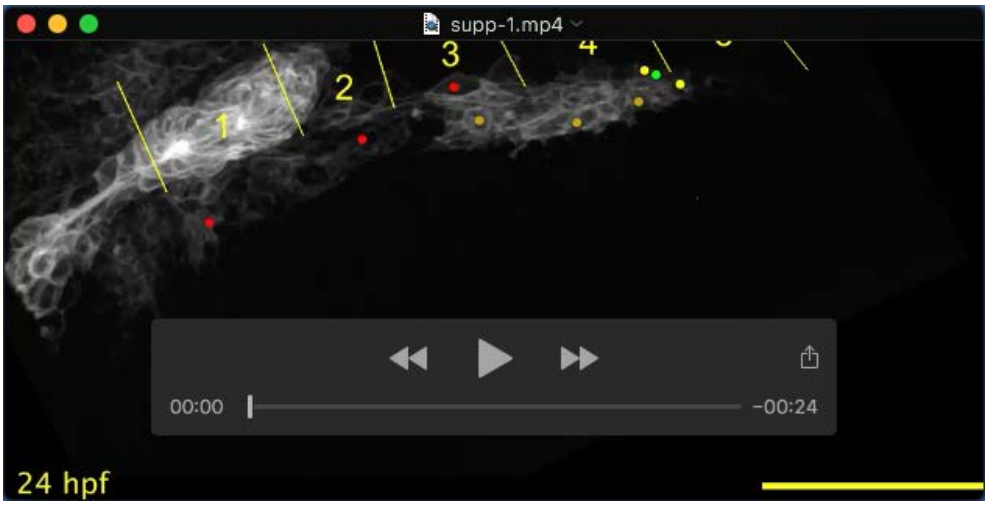

Movie 1. MMPs migrate away from the ventral edge of somites and generate the SHM, AbFM, AdFM, and PHM hypaxial muscles. Time-lapse imaging of MMPs in a transgenic embryo expressing the *six1b:lyn-GFP* transgene. Image is overlaid with manually-applied cell tracking dots, color-coded to indicate the muscle to which the tracked cell will contribute: SHM (red), AbFM (brown), AdFM (yellow), PHM (light blue), or the ventral extension from somite 6 (dark blue). Images were collected every 3 minutes from 24 to 60 hpf. Scale bar is 100 μm. This movie and Movie 2 are representative of 11 movies of varying lengths, and the cell tracking shown represents 53 cell lineages tracked for at least 80 timepoints each.

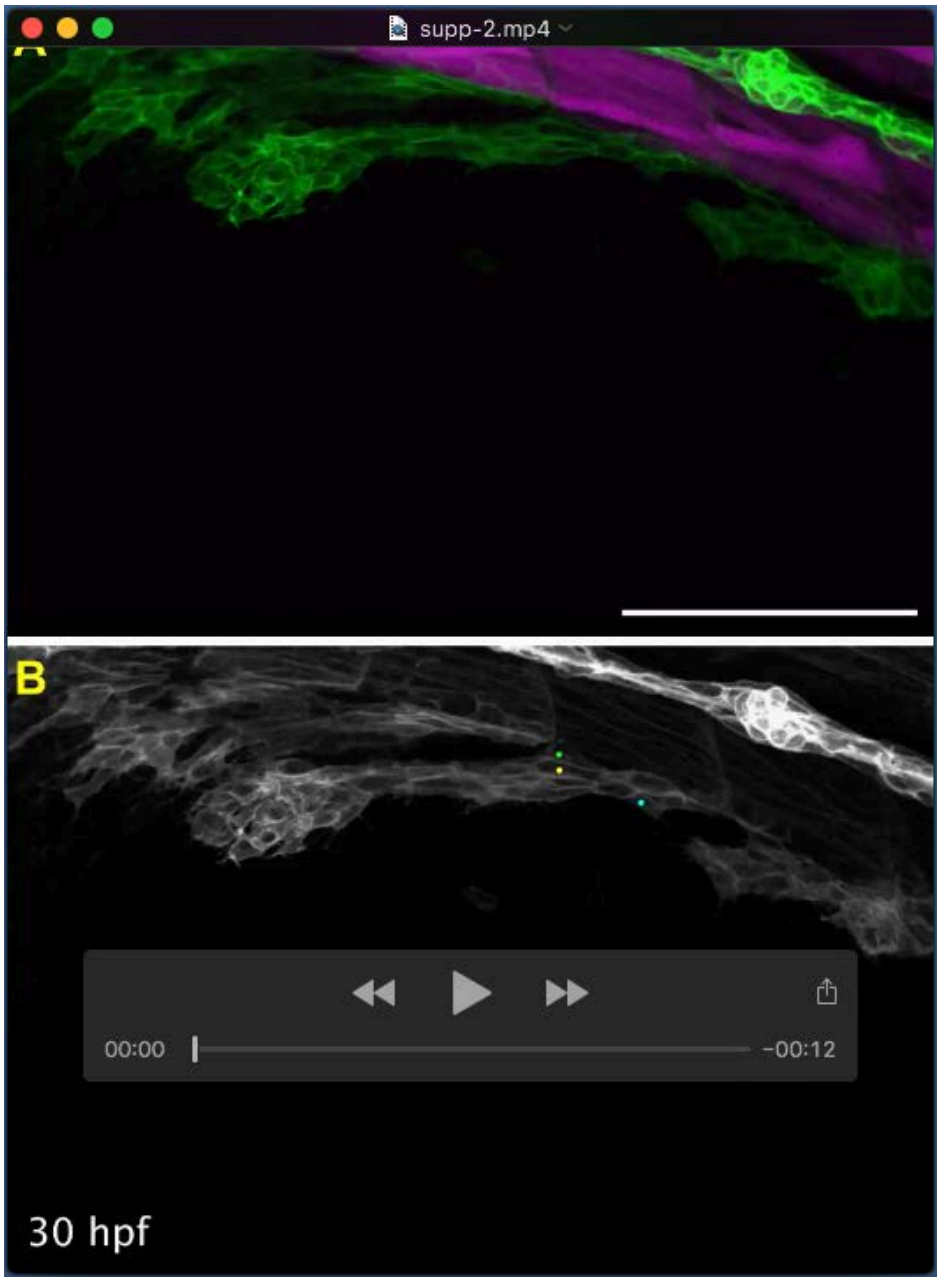

Movie 2. MMP migration at higher resolution. (A) Higher resolution time-lapse imaging of MMPs in a transgenic embryo expressing *six1b:lyn-GFP* (green) and *mylpfa:mCherry* (magenta) transgenes. (B) Isolated *six1b:lyn-GFP* channel, showing a cell lineage that contributes to the AdFM (yellow dots), one that contributes to the PHM (blue dots), and one that contributes to both the AdFM and the PHM (green dots). Images were taken every 5 minutes from 30-59 hpf. Scale bar is 100 μm.

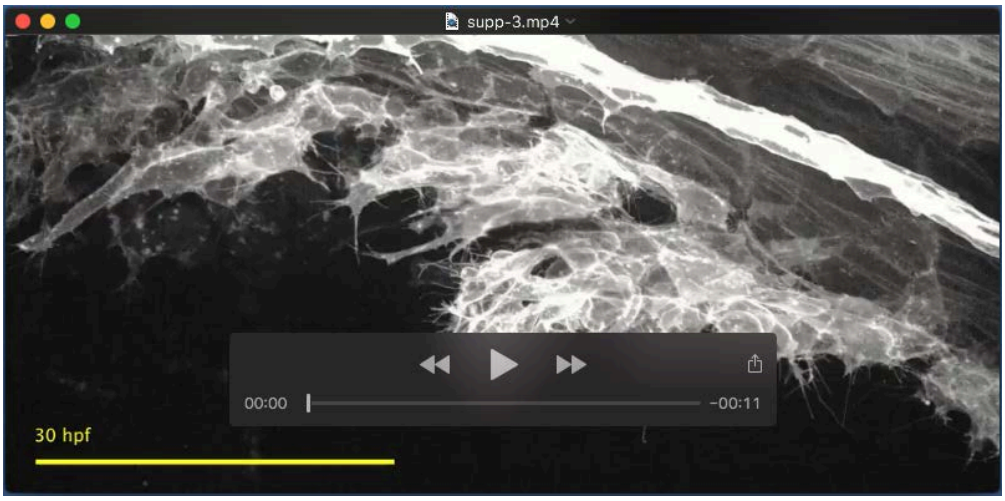

Movie 3. MMPs extend and retract long filopodia during migration. Time-lapse imaging of early MMP migration in a *six1b:lyn-GFP* transgenic embryo with high spatiotemporal resolution. Images were taken every 80 seconds from 30 to 37 hpf. At this resolution, long filopodia can be clearly seen extending and retracting from all MMPs. This time-lapse is representative of embryos imaged at this resolution (N=3). Scale bar is 100 μm.

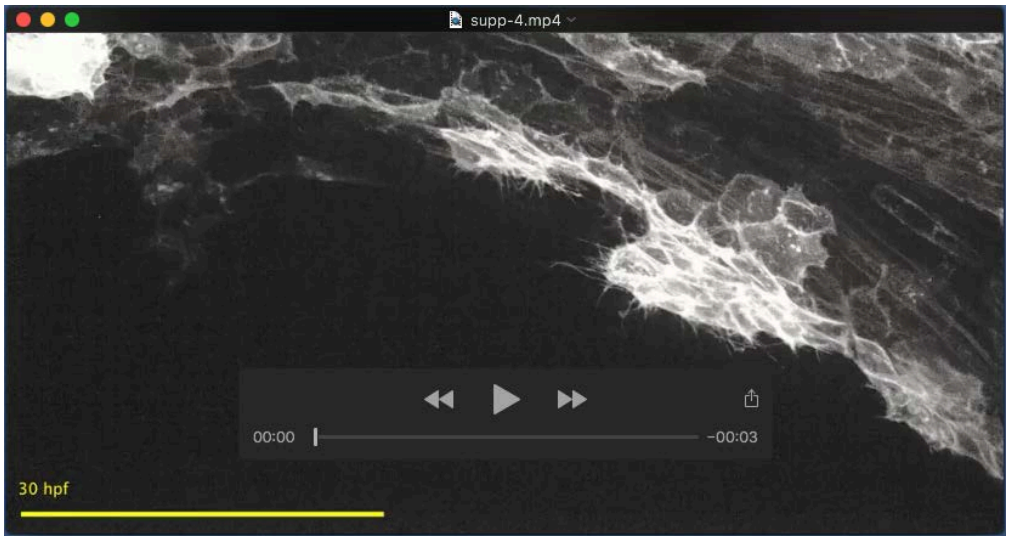

Movie 4. Early MMP migration in a *Δsix1a;4a;Δsix1b;4b* mutant embryo. High resolution time-lapse imaging of MMP-like cells in a *six1b:lyn-GFP* transgenic *Δsix1a;4a;Δsix1b;4b* mutant embryo. Although there is little to no cell migration, MMP-like cells extend and retract filopodia. Images are taken every 80 seconds from 30 to 32 hpf. This time-lapse is representative of embryos imaged (N=3). Scale bar is 100 μm.

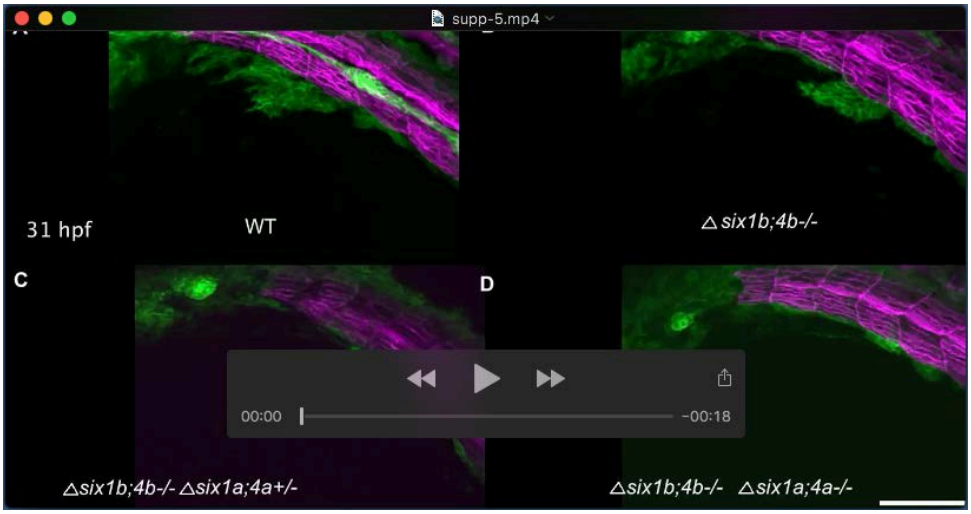

Movie 5. MMP migration is impaired in embryos with different combinations of *six1/six4* mutations. Time-lapse images of muscle growth and migration in (A) a wild-type embryo, (B) a *Δsix1b;4b* homozygote, (C) a Δ*six1b;4b* homozygote, also heterozygous for Δ*six1a;4a*, and (D) a *Δsix1a;4a;Δsix1b;4b* mutant. Images were taken every five minutes from 31 to 75 hpf. All embryos express *six1b:lyn-GFP* (green) transgene and the slow muscle transgene, *smyhc1:lyn-tdTomato* (magenta). Each panel is representative of at least two imaged embryos. Scale bar is 100 *μ*m and applicable to all panels.

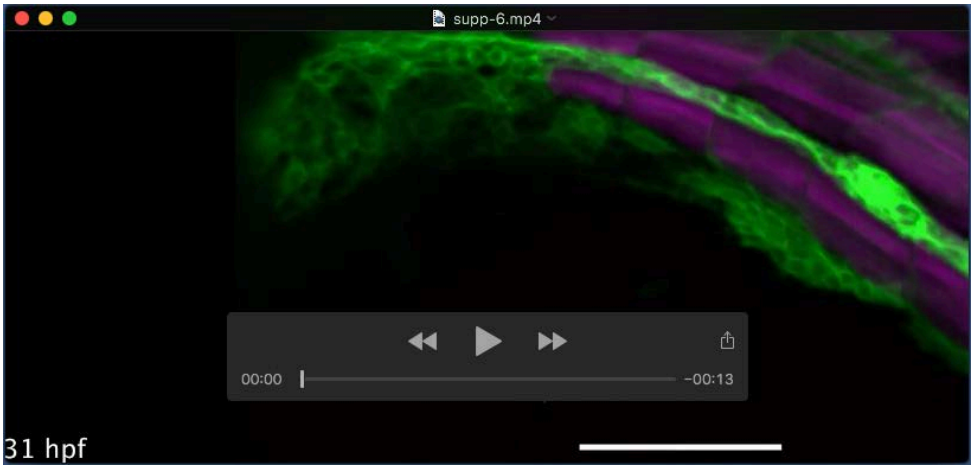

Movie 6. Met function is required for normal MMP migration. Time-lapse imaging of MMPs in a SGX523-treated embryo expressing *six1b:lyn-GFP* (green) and *mylpfa:mCherry* (magenta) transgenes. Although MMP streams form slowly, they mostly follow normal routes. However, within the fin bud, the AbFM fails to partition from the AdFM. Images were taken every 5 minutes from 31 hpf to 62 hpf. This time-lapse is representative of embryos imaged (N=3). Scale bar is 100 *μ*m.

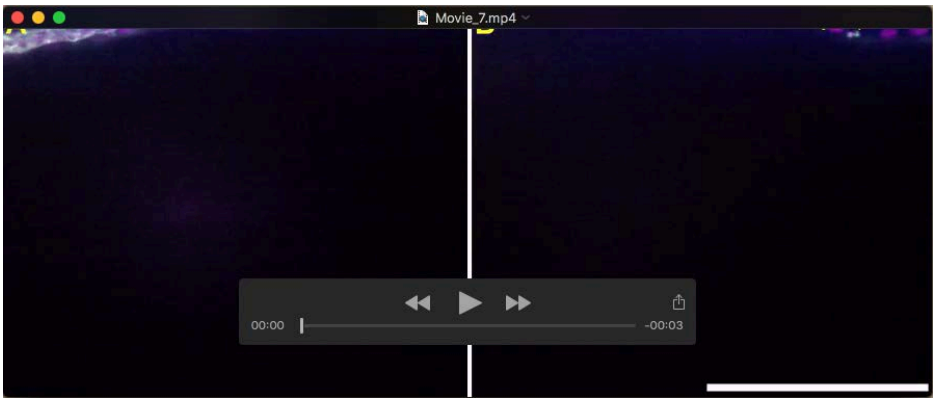

Movie 7. The AbFM is particularly affected by cyclopamine treatment. Confocal stack through embryos carrying *six1b:lyn-GFP* (mint), and *mylpfa:mCherry* (blue) that had been injected with mRNA encoding *H2B-CFP* (magenta); the fin bud outlines (yellow circles) are based on *H2B-CFP* label. Compared to (A) ethanol-treated control, the (B) cyclopamine-treated embryo has a small fin bud, with fewer MMPs than control. The difference is particularly apparent at the distal edge of the fin bud, where a large gap is present in the cyclopamine-treated embryo. Images in the confocal stack are spaced one micron apart. Scale bar is 100 μm.

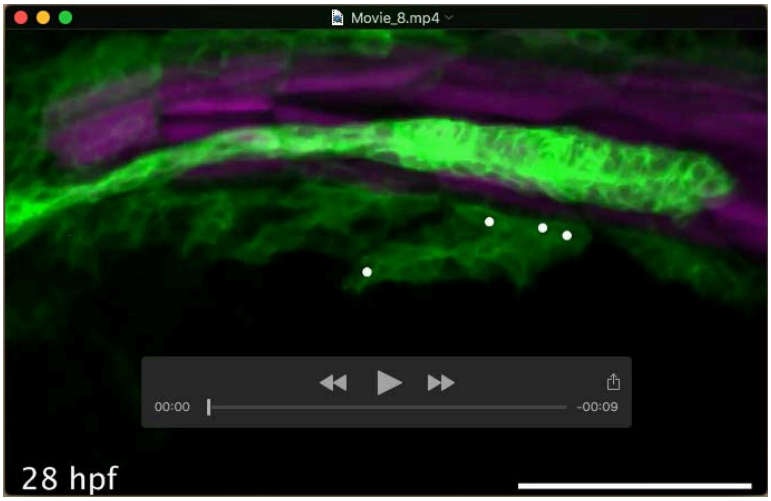

Movie 8. MMP migration and differentiation in an SU5402-treated embryo. Time-lapse imaging of MMPs in an SU5402-treated embryo expressing *six1b:lyn-GFP* (green) and *mylpfa:mCherry* (magenta) transgenes. MMPs from somite 4 initially migrate toward the region where the fin bud would normally form in a wild-type embryo, but subsequently contribute to the PHM. Cells are tracked from somite 4 (white dots and lines) to illustrate migratory routes. Images were taken every 5 minutes from 28 to 50 hpf. This time-lapse is representative of embryos imaged (N=5). Scale bar is 100 μm.